Article

Analysis of Lubrication Regimes for Porous Sliding Bearing

Aleksandar Marinković [1],*, Blaža Stojanović [2],*, Carsten Gachot [3] and Tatjana Lazović [1]

[1] Faculty of Mechanical Engineering, University of Belgrade, 11000 Beograd, Serbia; tlazovic@mas.bg.ac.rs
[2] Faculty of Engineering, University of Kragujevac, 34000 Kragujevac, Serbia
[3] Faculty of Mechanical and Industrial Engineering, Vienna University of Technology, 1040 Vienna, Austria; carsten.gachot@tuwien.ac.at
*   Correspondence: amarinkovic@mas.bg.ac.rs (A.M.); blaza@kg.ac.rs (B.S.)

Abstract: The purpose of this paper is to analyze the lubrication quality of porous sliding bearings, starting from the bearing model and in combination with experimental results aimed at analyzing the lubrication regimes of different working conditions. The separation between the surfaces by the lubricant layer is what determines the regime. The quality and type of lubrication regime are determined by parameters in the mathematical model including typically speed, load, motion, materials, environment, etc., which have an impact on friction. Besides those elements, important parameters such as coefficient of friction (COF) and working temperature are to be measured due to experimental investigations to detect an equilibrium working state. The self-lubrication mechanism in porous metal bearings improves their service life and lubrication processes; however, the COF still varies within a wide interval. This variability can be understood, considering that during bearing operation it operates within a broad range of lubrication regimes. Those findings are explained in the paper by using a combination of calculated parameters according to the bearing model and in combination with our own results of experimental investigations. With the obtained results for particular working conditions, the authors are trying to explain, in the form of a diagram with the limit line as an important outcome of the work, that the lubrication regime for porous metal bearings could arise from boundary lubrication (BL) close to hydrodynamic lubrication (HDL).

Keywords: lubrication regime; self-lubricating sliding bearing; oil film thickness; experimental investigation

1. Introduction and Lubrication Theory Background

Self-lubricated sliding bearings are very useful nowadays in numerous applications. There are two different types:

-   Sliding bearings that operate without the use of oil or grease. These bearings are made of special plastics, such as polymer-based composites with graphite or certain ceramic materials.
-   Sliding bearings that contain lubricants, either stored separately or within their own material structure. An example in this category is porous metal bearings, as a product of powder metallurgy, i.e., made by the sintering process [1]. Porous bearings are typically made from bronze, as a mixture of elemental powders of copper and tin, fully pre-alloyed bronze powder, or mixtures of these elements in addition to graphite as a solid lubricant. The pores in the material structure are filled with oil at the end of production. Such bearings do not require additional lubrication during their service life, representing their main advantage as maintenance-free supporting elements [2].

The first model for porous journal bearings, proposed by Morgan and Cameron [3], was based on a modified Reynolds equation, which considers the entry of the lubricant from the porous structure into the gap between the bearing and the journal. In a study on porous bearings lubrication, Cameron et al. [4] reported a relatively high coefficient of

friction (COF), despite the lubrication regime remaining fully hydrodynamic. They tried further to identify the critical threshold conditions for the transition from hydrodynamic to elastohydrodynamic and starved lubrication regimes. Murti [5] derived a modified Reynolds equation that takes into account the slip velocity effect and applies it to finite porous bearings. He concluded that the slip effect predominates at low permeability values. In order to conduct lubrication analysis, the authors of this paper started with basic parameters from the mentioned mathematical models [4], according to hydrodynamic lubrication (HDL) theory for porous metal bearings (Figure 1).
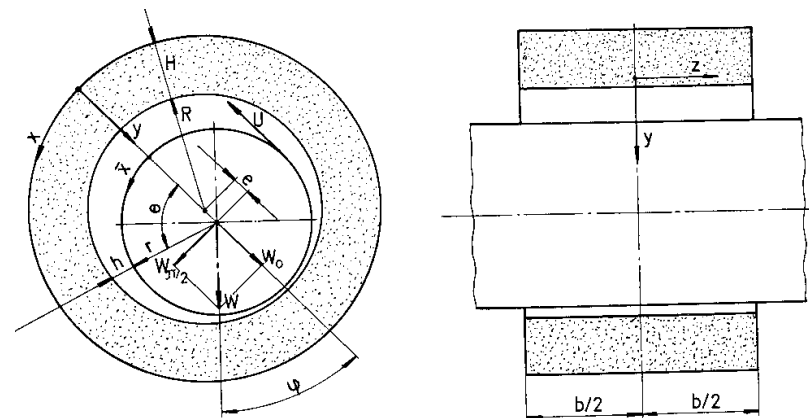

Figure 1. Model of self-lubricating porous metal bearing.

In this case, where we are talking about a short porous journal bearing [5], the theory explains that there is additional oil flow through the porous material of the bearing. This basic HDL theory of short porous bearings allows us to calculate and obtain some relationships between significant parameters, aimed to accomplish lubrication analysis as a goal. The results of numerical solutions of the oil film pressure expression yield several parameters and variables that could indicate the lubrication regime. The dimensionless design variable has significant importance and depends on material permeability Φ (in Darcys), bearing wall thickness H (in mm), and the clearance in bearing shaft interface c (in μm):

$$\Psi = \Phi H / c^3, \tag{1}$$

The main porous bearing loading characteristic, as for every sliding bearing, is doubtless Sommerfeld's number S defined by the relationship:

$$S = \frac{W}{U\eta b}\left(\frac{c}{r}\right)^2, \tag{2}$$

where W is the bearing radial load (in N), b is the bearing length (in mm), U is the peripheral speed (in m/s), r is the bearing/shaft radius (in mm), and η is the dynamic oil viscosity (in mPa s) for bearing lubrication. The results of the numerical solutions of the oil film pressure expression in the clearance of a short porous metal bearing [5] yield Ocvirk's loading parameter $S(d/b)^2$, (shown in Figure 2) and friction parameter $\mu\, r/c$ (presented in Figure 3). Both of those parameters depend on the design variable ψ and relative eccentricity ε calculated as $\varepsilon = e/c$.

Some authors have also tried to make a further step in HDL theory for this kind of bearing, dealing with different fluid flows in the journal–bearing gap. For example, the HDL of a porous bearing using the Reynolds modified equation under a turbulent regime and with slip velocity was analyzed by Kumar, etc. [6]. Prakash and Tiwari [7] analyzed the impact of the bearing–journal interface on lubrication quality. Their conclusion highlighted the strong impact of bearing surface roughness on both bearing performance and the lubrication regime. This influence may either amplify or diminish pressure build-up

depending on the bearing type, nominal geometry, roughness type, and working conditions of the contact.

In recent years, there have been several investigations published in papers which should be mentioned here, where authors study the lubrication regimes of porous bearings or sliding bearings in general. Paper [8] is focused on the phenomenon of lubrication regimes and their influence on the tribological characteristics of additively manufactured 316 steels within a novel lubrication environment. Furthermore, the curvature radius of wear traces (as indicated by the contact length) and their characteristics were examined. Finally, the impact of the curvature radius on the lubrication regime was assessed.
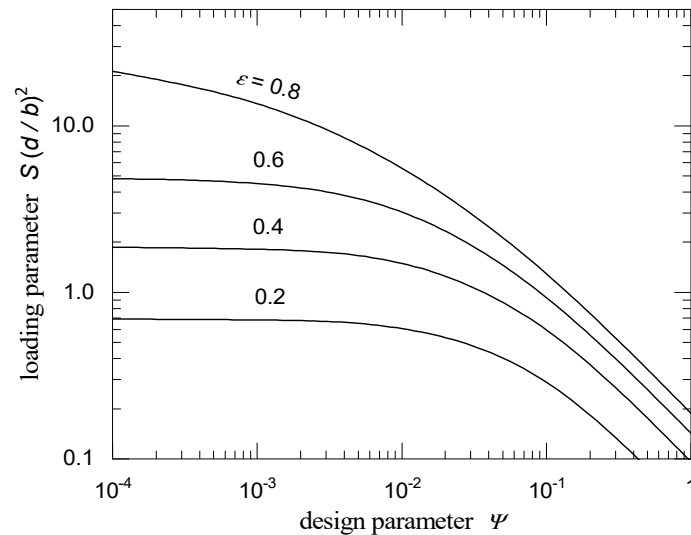
Figure 2. Loading parameter calculated values.
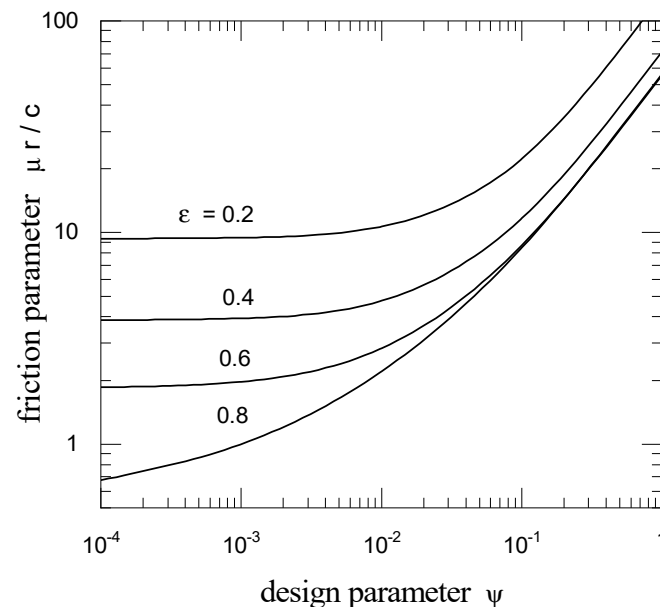
Figure 3. Friction parameter calculated values.

Various lubrication regimes can be distinguished based on the degree of surface separation. Proper lubrication of machine components enables uninterrupted and smooth operation, reduces wear, and prevents high strain or bearing failures [9]. This paper makes a significant contribution to the friction mapping methodology by highlighting the importance of sweep direction and its cumulative effect during running-in. In a broader

context, this is essential for the governing mechanisms that regulate film formation in elastohydrodynamic lubrication (EHL) contacts with rough surfaces.

Lubrication regime analysis supported by experimental results obtained in study [10] indicated that the correct selection of lubricant and suitable running conditions was very important in the tribological characteristics of porous bearings. In [11], the authors explored two different technological approaches to friction reduction within engines. The first solution is based on treating the active contact surfaces through the deposition of coatings, such as thin layers of amorphous carbon. The second solution is based on selecting a more effective lubricant, that has physicochemical properties other than its viscosity. This approach involves lubricants with additives. Additives are supposed to act when the lubricating film becomes insufficiently thick, avoiding direct metal-to-metal contact between rough surfaces. Specifically, the integration of anti-wear additives into the base lubricant emerges as a technological means to reduce both friction and wear rates, particularly within the mixed and boundary lubrication (BL) regimes. The current findings could be beneficial for automotive engine designers to improve the performance characteristics of crankshaft bearings.

The authors of paper [12] calculated the oil film pressure and thickness of the sliding bearing in a low-speed rotor system under various torque loads. They simulated these loads measured from a bearing load sensor and determined the lubrication state of the sliding bearing under torque loads based on the film thickness ratio. Consequently, they established a direct relationship between torque loads and lubrication conditions. The research findings presented in this paper give significant guidance for adjusting the actual working conditions of sliding bearings and predicting their life.

According to the above-mentioned references concerning the background of lubrication theory, the authors of this paper are trying to support calculations of regime analysis parameters and observations using the results of their experimental investigations, which could be a modest contribution and possible added value to this field, including the lubrication limit line diagram that will be further explained in the discussion.

2. Experimental Investigations

Possibly the first authors to experimentally investigate porous bearings to improve certain parameters using a theoretical model were Cusano and Phelan. The results presented in [13] confirm the functionality of porous bearings at high eccentricity ratios and demonstrate the correlation of permeability effects with load-carrying capability. These contributions were highly significant for the development and numerical modeling of porous bearings.

A lot of experimental investigations and experience from exploitation showed that porous bearings work mostly under boundary lubrication and mixed lubrication. Further analysis is an attempt to provide proof that the lubrication regime could also become very close to hydrodynamic, probably more akin to elastohydrodynamic lubrication. Using their experimental results, with the already mentioned numerical model [4,5], the authors try to explain that only at higher speeds and lower radial bearing loads could such a lubrication regime eventually appear with no contact at the journal–bearing interface.

Experiments were conducted in the machine design laboratory on a test rig USL 5-30 for sliding bearings [14]. The testing bench is shown in Figure 4, with its main components and bearing samples. Testing samples were made from two different materials: bronze CuSnlO and bronze with 1% graphite powder addition in the basic bronze material (CuSnlO + l%C). The main physical performances of those bearing materials are shown in Table 1, with probe dimensions of $\varnothing 20/\varnothing 30 \times 20$ mm (shown in Figure 4a).

For the sinter metal bearings, synthetic oil FAMGEN KL3 was applied. This is a thermally stable, synthetic lubricating oils used for sinter products and chain lubrication. This lubricant contains additives that enable excellent load-bearing capacity and the creation of extremely adhesive lubricating film. At the end of production, porous metal bearings with a porosity of about 20% are filled with the aforementioned synthetic oil. Under

vacuum conditions, every sintered bearing sample can be filled by approx. 80% of its volume, where only blind pores in the original sintered matrix remain oil-free and useless in the well-understood lubrication mechanism. FAMGEN KL-3 synthetic oil is applicable in a wide temperature interval from $-35\,°C$ up to $+220\,°C$, with good-enough thermal stability as an important characteristic. According to ISO 3104:2023 standard [15] and ISO 2909:2002 standard [16], lubricant producers reported these synthetic oil tribo-chemistry performances: density of $920\,kg/m^3$, kinematic viscosity of $30\,mm^2/s$ at $40\,°C$, and 140 as a viscosity index value.

(**a**)   (**b**)
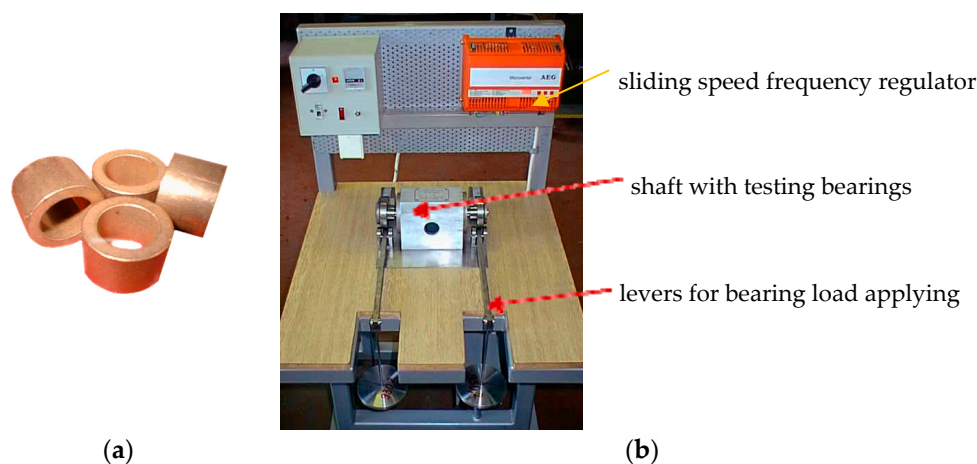
Figure 4. (**a**) Tested bearing samples and (**b**) USL 5-30 test bench for self-lubricating bearings.

Table 1. Materials and their properties of tested bearing samples.

Property/Material	CuSn10	CuSn10 + 1% C
Density, g/cm^3	6.45 ± 0.05	6.56 ± 0.02
Open porosity, %	22.81 ± 0.36	18.8 ± 0.5
Max radial force, N	3550 ± 50	1825 ± 75
Hardness, HB	34.75 ± 1.49	34.5 ± 1.5

The above-detailed bearing samples were tested under nine different working conditions, where sliding speed was in an interval of $v = (1...5)\,m/s$ with the corresponding bearing load values determined according to a pv range limit, which should be in an interval of $W = (750...150)\,N$. Standard laboratory environmental conditions were common for this kind of investigation, with air temperature $20 \pm 1\,°C$ and relative humidity $(40...70)\%$ for the whole time during the experiments.

By utilizing the test rig (Figure 4b), it is possible to enhance the setup by integrating a portable NI DAQ system (Figure 5). The primary rationale for employing the DAQ system in these measurements is the necessity of simultaneously testing two samples, which requires monitoring two channels for friction torque and bearing temperature concurrently [17]. Here it should be explained that friction torque comes from bending lever stress under the corresponding bearing load. This is further transformed by DNS and presented as the COF value of the bearing, following its trend over time via the LabVIEW application. The same acquisition and thermocouple were used to follow the working temperature value over time. It was not necessary to apply a high sample rate for this kind of experiment since the advantages of obtaining results by DAQ and its availability for further analyses are evident.
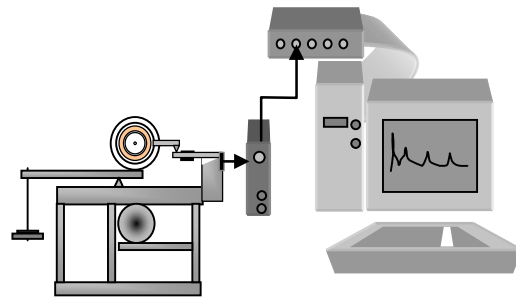
Figure 5. DAQ support scheme for experiments with test bench for self-lubricating sliding bearings.

3. Results and Lubrication Regime Discussion

The first observation in all numerous experimental investigations shows that current bearing temperature and the COF values of porous metal bearings were noted until they become a constant, which takes about 40 to 60 min from the start of the experiment. This experimental investigation shows that the dependence of those two working parameters over time can be the best polynomial approximation [14]. The results in Figure 6 represent this trend for only a single combination of working conditions in an investigation, here for higher speed (v = 5 m/s and load W = 170 N). In addition to these, numerous tests were performed under other working conditions and they show a similar trend of bearing temperature and COF results, considering that the time from the start of the experiment needs to approach equilibrium values. Following the temperatures and COF trends in Figure 6, one can observe that the higher values of those parameters relate to the porous bronze material CuSn with a graphite addition (+1% C) under the same working conditions. This could be explained by the fact that the graphite addition affects a better COF for lower sliding velocities, especially in intervals where v = (1...2) m/s. For the highest sliding speed, this may not follow such a trend, as shown in Figure 6. On the other hand, the addition of the graphite in the porous matrix can lead to a more comfortable lubrication regime, as will be shown in the later discussion.
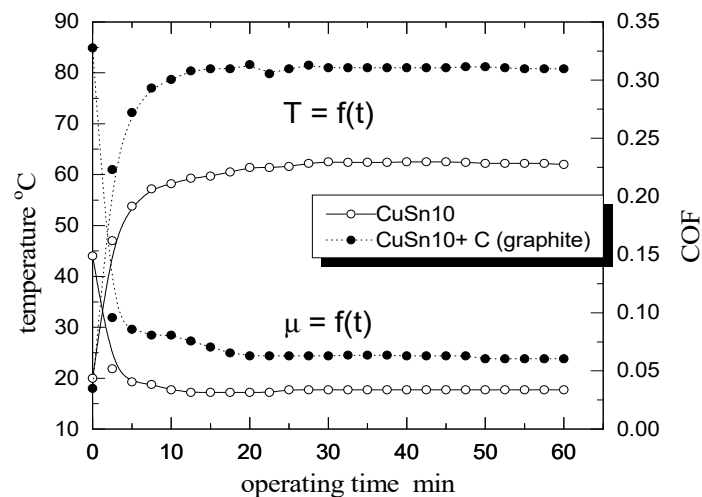

Figure 6. Bearing temperature and COF trend due to a time (parameters v = 5 m/s and W = 170 N).

The mentioned mathematical model and calculations regarding lubrication quality, when combined with results obtained from experimental investigations, allow for a comprehensive analysis of the sliding bearing lubrication regime and its determination. It is undeniable that lubrication quality and the COF value depend on the bearing surface quality, with special consideration given to the porous material characteristics that significantly influence bearing behavior during operation. Therefore, the initial step in this process must focus on analyzing the bearing surface/profile. This analysis was conducted

on a bearing segment both before and after an exploitation period. Through collaboration with the Competence Center for Tribology (AC2T) in Wiener Neustadt, Austria, and their testing equipment, it was very interesting and useful to observe the bearing sample (CuSn with a 1% graphite addition) surface segment scanned and profile measured before the experiments (Figure 7). The scan revealed numerous channels within the porous material structure, originating from open pores on the surface and extending into the bulk of the bearing, with some reaching depths of nearly 0.1 mm from the surface. But after only several hours of exploitation (needed in a wear rate investigation), under the above-described working conditions (Figure 6), it is interesting to compare with the starting case and observe clear differences in the sample's material surface. In Figure 8, the bearing segment surface profile after exploitation indicates that the pores situated directly on or near the surface were nearly closed due to the load and sliding processes at the interface. Deep pores are no longer present, leaving a bearing surface with a roughness of less than 10 μm, suggesting that pores at the interface are closing during further exploitation. This phenomenon occurs in the starting period of work and doubtless could have a significant impact in defining the lubrication regime. It could be positive from the side of the lubrication regime because the closing of the pores in the area where the load is greatest leaves the lubricant in that zone and reduces the outflow of oil through the pores in a matrix, which can improve lubrication and thereby bring it closer to the limit line towards HDL.
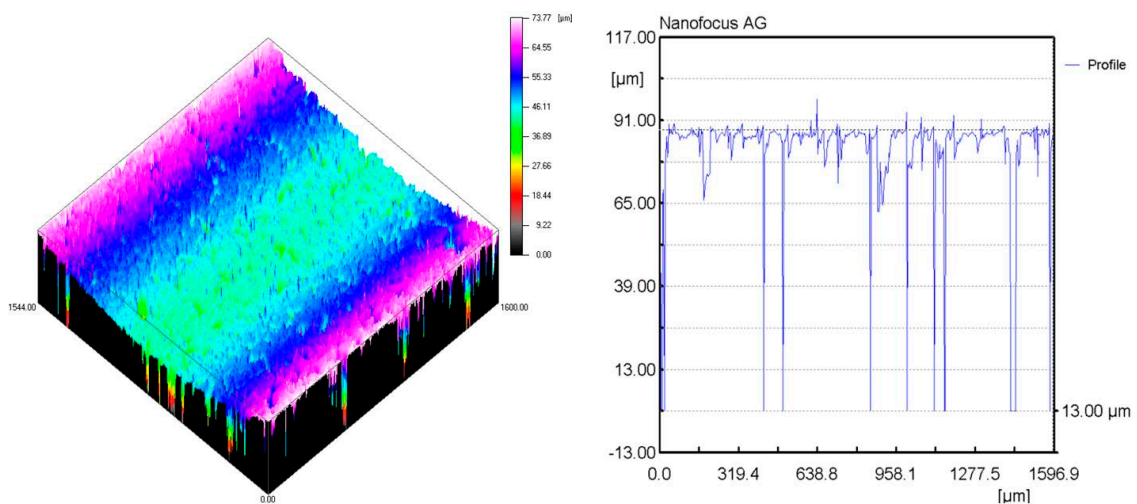

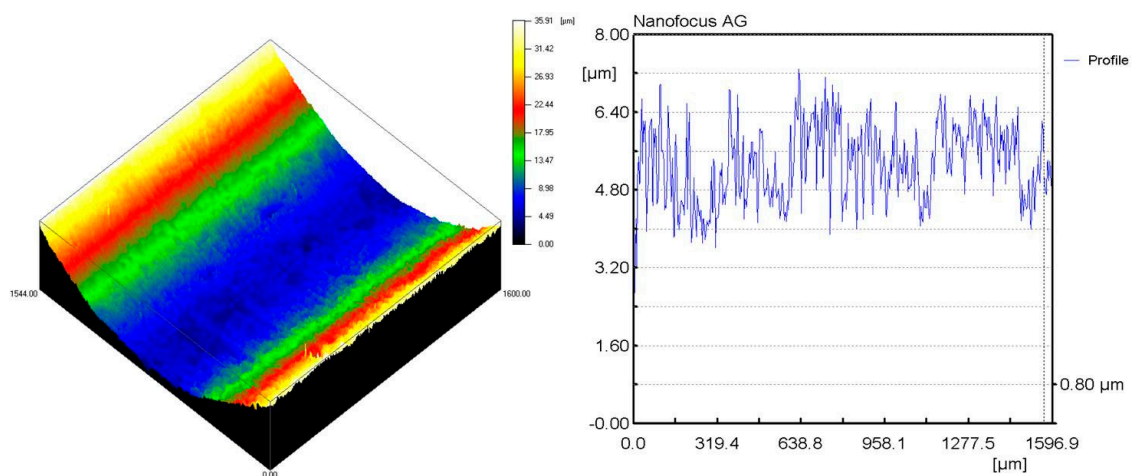**Figure 7.** Bearing segment and contact surface profile—before experiments.

Figure 8. Bearing segment and contact surface profile—after experiments.

To determine and compare lubrication quality across various sliding speeds and load variations, experimental investigations were conducted under nine different working parameters for both mentioned bearing materials. These conditions (see Table 2) were selected to cover a sliding speed range of 1 to 5 m/s and load variations up to 2 N/mm^2 pressure, as these are the most common conditions encountered in the service life of porous sliding bearings used in industries such as automotive and household appliances. Considering the available number of samples, as well as the validity of the experiments with an acceptable measurement error, for each of the selected working conditions, 20–30 tests were performed with appropriate previously run-in samples.

Table 2. Experimental results with working conditions and parameters for analysis.

Working Condition No.	Material	v	p	Viscosity η	1/S	Design Variable ψ	Equilib. Temp. T	Equilib. COF
		m/s	N/mm^2	Pa s	-	-	°C	-
1	CuSn	1.03	1.93	0.01	0.085	0.09	70 ± 2	$0.03 \pm 1\%$
	CuSn + 1%C	1.03	1.93	0.011	0.093	0.45	69 ± 2	$0.02 \pm 1\%$
2	CuSn	1.19	1.68	0.011	0.124	0.15	75 ± 2	$0.03 \pm 1\%$
	CuSn + 1%C	1.19	1.68	0.013	0.147	0.50	68 ± 2	$0.02 \pm 1\%$
3	CuSn	1.29	1.55	0.013	0.172	0.26	76 ± 2	$0.025 \pm 1\%$
	CuSn + 1%C	1.29	1.55	0.013	0.172	0.55	66 ± 2	$0.02 \pm 1\%$
4	CuSn	1.41	1.42	0.013	0.205	0.35	77 ± 2	$0.025 \pm 1\%$
	CuSn + 1%C	1.41	1.42	0.013	0.205	0.60	70 ± 2	$0.025 \pm 1\%$
5	CuSn	1.72	1.16	0.012	0.283	0.42	75 ± 2	$0.025 \pm 1\%$
	CuSn + 1%C	1.72	1.16	0.013	0.307	0.65	70 ± 2	$0.025 \pm 1\%$
6	CuSn	2.22	0.96	0.011	0.431	0.52	72 ± 2	$0.025 \pm 1\%$
	CuSn + 1%C	2.22	0.96	0.012	0.472	0.70	72 ± 2	$0.030 \pm 1\%$
7	CuSn	3.10	0.64	0.009	0.694	0.60	68 ± 2	$0.025 \pm 1\%$
	CuSn + 1%C	3.10	0.64	0.010	0.769	0.70	75 ± 2	$0.03 \pm 1\%$
8	CuSn	3.88	0.52	0.009	1.07	0.68	66 ± 2	$0.025 \pm 1\%$
	CuSn + 1%C	3.88	0.52	0.010	1.19	0.75	75 ± 2	$0.04 \pm 1\%$
9	CuSn	5.17	0.39	0.008	1.69	0.76	65 ± 2	$0.03 \pm 1\%$
	CuSn + 1%C	5.17	0.39	0.009	1.9	0.85	76 ± 2	$0.05 \pm 1\%$

The results from those experiments were used to calculate bearing parameters of importance for lubrication, previously explained in the lubrication theory background section. The significant data for lubrication mentioned here are the relative bearing length of samples $b/d = 1$ and the samples' relative wall thickness $H/d = 0.25$. Concerning clearance values, these were $c = (9\ldots11)$ μm for all treated bearing samples, while relative clearance takes values were in the range of $c/r = (0.9\ldots1.1) \times 10^{-3}$. Regarding different material properties, the calculated permeability values were $\Phi = (0.044\ldots0.053)$ Darcys for the pure bronze samples (CuSn), and for bronze with a graphite addition (CuSn + 1%C) the permeability values were in the interval $\Phi = (0.018\ldots0.026)$ Darcys. The corresponding bearing design parameters were also calculated for the bronze samples (CuSn) as $\psi = (0.09\ldots0.76)$, but for the sintered material with a graphite addition (CuSn + 1%C) they were in the range $\psi = (0.45\ldots0.85)$.

Sommerfeld's number S and the design variable ψ were calculated (see Table 2) and plotted as points in the diagram (Figure 9), where the regime limit line ($\varepsilon = 1$) separates the areas of HDL and BL [4]. Lubrication is at least very close to hydrodynamic, but only at the highest sliding velocity values (working conditions Nos. 7, 8, and 9 in Table 2). Other studies investigating the elastic deformations bearings [14] provide arguments suggesting that these approach some form of EHL, which is close to the lubrication limit line. On the other hand, under lower velocities and higher loads (working conditions Nos. 1 to 5 in

Table 2), we can doubtless identify only BL, where the lubrication film thickness is at its lowest, not even approaching the limit line.
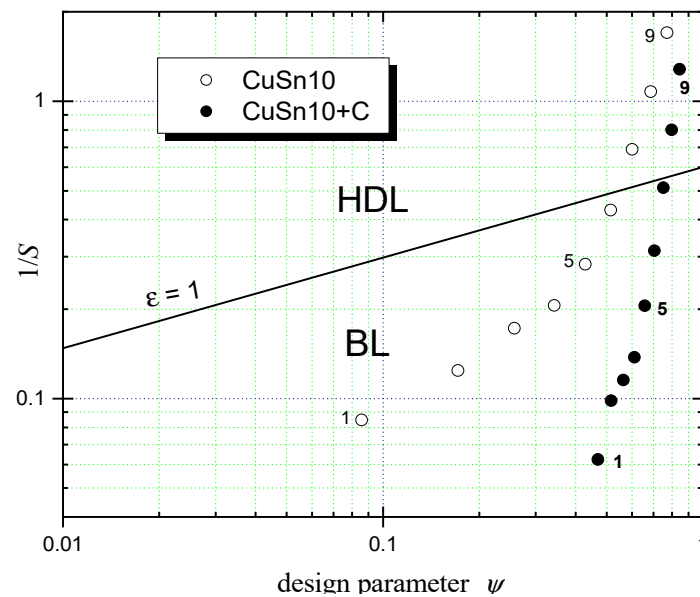

Figure 9. Working condition points with the lubrication regime limit line ($\varepsilon = 1$).

The above-mentioned observations could be also indicated through the relative oil film thickness, calculated by oil film thickness:

$$\lambda = \frac{h_{\min}}{\left(R_{q_1}^2 + R_{q_2}^2\right)^{1/2}} \tag{3}$$

The oil film thickness value is calculated as $h_{\min} = c\,(1 + \varepsilon \cos\theta)$, for a minimum value of angle $\theta = \pi$, where parameter ε represents the relative eccentricity of the bearing. The root mean square deviation of the contact surface roughness (RMS) was measured for the bearing–shaft interface before the experimental investigations. It was determined as $R^2{}_{q1} = 0.30 \pm 0.01$ μm of the profile values for the shaft. Another element in the interface represents a bearing surface with a roughness (RMS profile value) for the bronze (CuSn) bearing of $R^2{}_{q2} = 2.5 \pm 0.5$ μm and for the other bushing material with a graphite addition (CuSn + 1% C) this was $R^2{}_{q2} = 3.5 \pm 0.5$ μm [14].

The COF calculated based on HDL theory, combined with experiments and the calculation of relative oil film thickness λ, could indicate the type of lubrication expected under corresponding working conditions. According to the data in Table 3, one could conclude and confirm that the investigation of porous bearings for both materials was mostly working under the regime of BL. Just for the highest values of sliding velocity (points 8 and 9 in Figure 9) can we talk about the lubrication coming close to the hydrodynamic. The calculated values of relative oil film thickness λ in Table 3 also confirm this observation, showing that even for the highest sliding velocities the lubrication regime is not clearly hydrodynamic, where in such a case it should be $\lambda > 5$. The best qualities of those bearing lubrications could be approached only in case of a high enough clearance, for samples of porous bronze CuSn or those with a graphite addition (CuSn + 1% C), combined with the higher sliding speed ($v \approx 5$ m/s). The analyzed parameters and facts could give proper support for further EHL study of the sliding bearing [18].

Table 3. Relative oil film thickness values for key lubrication modes.

Working Condition No.	→	ε	h_{min}, μm	λ	μ r/c
7	CuSn	-	-	-	-
	CuSn + 1%C	0.80	2.0	0.57	8.5
8	CuSn	-	-	-	-
	CuSn + 1%C	0.60	4.0	1.14	8.5
9	CuSn	0.79	2.1	0.83	17
	CuSn + 1%C	0.38	6.2	1.76	12

4. Conclusions

The specific way of operating self-lubricating sliding bearings makes the lubrication process better compared with classical sliding bearings, even though its COF in exploitation still varies across wide intervals. This can be understood if we know that during the life of a bearing it works in regimes from boundary lubrication to hydrodynamic lubrication. Numerous conducted experimental investigations and experience from exploitation have shown that porous metal bearings are working under boundary and mixed lubrication for most of their life cycle. Only at higher sliding speed ($v \approx 5$ m/s) and corresponding lower radial loads ($W \approx 150$ N), could we suppose that lubrication could come closer to hydrodynamic lubrication, which means approaching an area ($\varepsilon = 1$) near the lubrication limit line (Figure 9). This kind of lubrication regime could indicate that there is no surface contact between the shaft and the bearing, which is the best situation in sliding bearing exploitation. This analysis and explanation could be interesting and useful for further investigation of this kind or similar bearings. The study conducted in this paper, along with the presented results, could indicate a few implications for applications and practice. Even though every tribosystem is specific and there is no universal recipe for sliding bearing selection, bearing designers and engineers could use the information presented in this paper as some kind of guide or advice on how to select proper porous bearing materials (with or without corresponding solid lubricants). Following specific working parameters (load and speed), this proper selection aims to achieve the desirable quality of bearing lubrication, to approach as near as possible to the optimal lubrication regime. Looked from another perspective, that of bearing consumers, these results and the analysis following optimization procedures (not mentioned in this topic) could help in proper interface (bearing–lubricant–shaft) selection for particular working conditions faced in exploitation. In some specific cases, it could be concluded that porous bearings should be replaced by polymer or some controllable and active sliding bearings [19], since those also have some advantages.

Author Contributions: Conceptualization, A.M., B.S., and C.G.; methodology, A.M., B.S., and C.G.; validation, A.M., B.S., and T.L.; investigation, A.M. and T.L.; writing—original draft preparation, A.M. and T.L.; writing—review and editing, A.M., B.S., and C.G.; visualization, A.M., B.S., and T.L.; supervision, A.M. and C.G. All authors have read and agreed to the published version of the manuscript.

Data Availability Statement: The raw data supporting the results, discussion and conclusions of this article will be made available by the authors on request.

Conflicts of Interest: The authors declare no conflicts of interest.

References

1. Cheng, J.A.; Lawley, A.; Smith, W.E.; Robertson, J.M. Structure property and performance relations in self-lubricating bronze bearings: Commercial premixes. *Int. J. Powder Metall. Am. Powder Metall. Inst. Int.* **1986**, *22*, 149–162.
2. Morgan, V.T. The Applications of porous metal bearings. *Ind. Lubr. Tribol. Emerald Insight* **1972**, *24*, 129–138. [CrossRef]

3. Morgan, V.T.; Cameron, A. Mechanism of lubrication in porous metal bearings. In Proceedings of the Conference of Lubrication and Wear, Institution of Mechanical Engineers, London, UK, 1–3 October 1957; Proceedings paper 89. pp. 151–157.
4. Cameron, A.; Morgan, T.V.; Stainsby, E.A. Critical Conditions of Hydrodynamic Lubrication of Porous Metal Bearings. *Proc. Inst. Mech. Eng.* **1960**, *176*, 761–770.
5. Murti, P.R.K. Hydrodynamic lubrication of short porous bearings. *Wear* **1972**, *19*, 17–25. [CrossRef]
6. Kumar, W. Porous Metal Bearings—A critical Review. *Wear* **1980**, *63*, 271–287. [CrossRef]
7. Prakash, J.; Tiwari, K. Lubrication of a porous bearing with surface corrugations. *Trans. ASME J. Lubr. Technol.* **1982**, *104*, 127–134. [CrossRef]
8. Korkmaz, M.E.; Gupta, M.K.; Demirsoz, R. Understanding the lubrication regime phenomenon and its influence on tribological characteristics of additively manufactured 316 Steel under novel lubrication environment. *Tribol. Int.* **2022**, *173*, 107686. [CrossRef]
9. Hansen, J.; Bjorling, M.; Larsson, R. Mapping of the lubrication regimes in rough surface EHL contacts. *Tribol. Int.* **2019**, *131*, 637–651. [CrossRef]
10. Durak, E. Experimental Investigation of Porous Bearings Under Different Lubricant and Lubricating Conditions. *KSME Int. J.* **2003**, *17*, 1276–1286. [CrossRef]
11. Hamel, R.; Lahmar, M.; Bou-Said, B. Elasto-hydrodynamic lubrication analysis of a porous misaligned crankshaft bearing operating with nanolubricants. *Mech. Ind.* **2023**, *24*, 2. [CrossRef]
12. Pang, X.; Jiang, W.; Jin, X. Investigation on Lubrication State of Sliding Bearings in Low-Speed Rotor System Subjected to Torque Load. *Int. J. Rotating Mach.* **2019**, *2019*, 1791830. [CrossRef]
13. Cusano, C.; Phelan, R.M. Experimental investigation of porous bronze bearings. *Trans. ASME J. Lubr. Technol. Ser. F* **1973**, *95*, 173–180. [CrossRef]
14. Marinković, A.; Lazović, T.; Stanković, M. Experimental investigations of porous metal bearings. In Proceedings of the 15th International Conference on Experimental Mechanics, Porto, Portugal, 22–27 July 2012; Proceedings paper 2718. pp. 1–6.
15. *ISO 3104:2023*; Petroleum Products—Transparent and Opaque Liquids—Determination of Kinematic Viscosity and Calculation of Dynamic Viscosity. ISO: Geneva, Switzerland, 2023.
16. *ISO 2909:2002*; Petroleum Products—Calculation of Viscosity Index from Kinematic Viscosity. ISO: Geneva, Switzerland, 2002.
17. Marinković, A.; Vencl, A.; Wallace, P. Portable DAQ equipment with LabVIEW as a tool for tribology experiments and condition monitoring. In Proceedings of the 10th International Conference on Tribology Serbiatrib '07, Kragujevac, Serbia, 19–21 June 2007; pp. 105–108.
18. Wei, L.; Wei, H.; Duan, S.; Zhang, Y. An EHD-mixed lubrication analysis of main bearings for diesel engine based on coupling between flexible whole engine block and crankshaft. *Ind. Lubr. Tribol.* **2015**, *67*, 150–158. [CrossRef]
19. Santos, F.I. Controllable Sliding Bearings and Controlable Lubrication Principles—An Overview. *Lubricants* **2018**, *6*, 16. [CrossRef]